Supporting Information

Regulating coordination environment of metal-organic frameworks for efficient electrocatalytic oxygen evolution reaction

Enjun Lv[1], Jiayi Yong[1], Jinguli Wen[1], Zhirong Song[1], Yi Liu[2], Usman Khan[1*], Junkuo Gao[1*]

[1]Institute of Functional Porous Materials, School of Materials Science and Engineering, Zhejiang Sci-Tech University, Hangzhou 310018, China

[2]Institute for Composites Science Innovation, School of Materials Science and Engineering, Zhejiang University, Hangzhou 310027, People's Republic of China

Corresponding Author

Usman Khan: usman.cssp@hotmail.com

Junkuo Gao: jkgao@zstu.edu.cn

Experimental Section

1.1 Chemicals

$Fe(NO_3)_3 \cdot 9H_2O$, $Co(NO_3)_2 \cdot 6H_2O$, and KOH were purchased from Aladdin Ltd. (Shanghai, China). 2,5-dihydroxyterephthalic acid (L_1) and 4,6-dihydroxyisophthalic acid (L_2) were purchased from Extension (China). N, N-dimethyl formamide (DMF), isopropanol and ethanol were purchased from Macklin (Shanghai, China). Nafion was purchased from Alfa Aesar (China). Ag/AgCl electrode,

modified glassy carbon electrode, and carbon electrode were purchased from Gaoss Union (Wuhan, China). All chemicals were used without further purification. Deionized water was used throughout the experiment.

1.2 Material synthesis

According to the published literature[1], FeCo-L_1 and FeCo-L_2 were prepared. In detail, 30 mg (0.15 mol) of L_1 was dissolved in 5 ml DMF and stirred until completely dissolved. 97 mg (0.24 mol) $Fe(NO_3)_3 \cdot 9H_2O$ and 70 mg (0.24 mol) $Co(NO_3)_2 \cdot 6H_2O$ were dissolved in 5 ml DMF and stirred until completely dissolved. Then, the metal ion solution was added to the L_1 ligand solution, 0.6 ml of deionized water was added dropwise, and the mixed solution was transferred to the polytetrafluoroethylene hydrothermal reactor. The solvothermal reaction was carried out for 24 hours at a temperature of 120 °C. The reaction product was washed with DMF and ethanol and dried in a vacuum oven at 60 °C for 6 hours. The final powder sample obtained is FeCo-L_2. Using ligand L_2 instead of ligand L_1, FeCo-L_2 could be prepared by the same method.

Dissolve 15 mg (0.075 mol) L_1 and 15 mg (0.075 mol) L_2 in 5 ml DMF and stir until completely dissolved. 97 mg (0.24 mol) $Fe(NO_3)_3 \cdot 9H_2O$ and 70 mg (0.24 mol) $Co(NO_3)_2 \cdot 6H_2O$ were dissolved in 5 ml DMF and stirred until completely dissolved. Then, the metal ion solution was added to the ligand solution, 0.6 ml of deionized water was added dropwise, and the mixed solution was transferred to the polytetrafluoroethylene hydrothermal reactor. The solvothermal reaction was carried out for 24 hours at a temperature of 120 °C. The reaction product was washed three times with DMF and ethanol and then dried in a vacuum oven at 60 °C for 6 hours. The final powder sample obtained is FeCo-L_1L_2. Changing the ratio of metal ions Fe and Co or the ratio of ligands L_1 and L_2 can prepare different ratios of FeCo-L_1L_2.

1.3 Characterization

The morphologies of the samples were observed by field-emission scanning electron microscopy (FE-SEM, Vltra55, Carl Zeiss) with transmission electron microscopy (TEM, JEM-2100). The powder X-ray diffraction (XRD) was recorded on a Bruker D8

Advance diffractometer with a Cu Ka radiation. The functional groups of the samples were demonstrated by Fourier transform infrared (FT-IR, Nicolet 5700, Thermo Electron). X-ray photoelectron spectroscopy (XPS) data were obtained by Thermal Fisher Scientific K-Alpha electron spectrometer.

1.4 Electrochemical testing

Electrochemical measurements were performed with a Zahner Zennium electrochemical workstation using a typical three-electrode setup with a 1.0 M KOH aqueous solution electrolyte solution. The Ag/AgCl electrode is used as the reference electrode in the three-electrode system. The glassy-carbon electrode (GCE, geometric area: 0.07 cm^2) is used as the working electrode, and the carbon electrode is used as the counter electrode. For the fabricated electrode, 5 mg sample, 250 μL isopropanol, 750 μL deionized water and 30 μL Nafion were mixed and dispersed by ultrasonic for 30 min. Next, 5 μL of catalyst ink was dropped on the glassy-carbon electrode and air drying for 2 hours at least. First, perform continuous cyclic voltammograms (CV) testing at a scan rate of 500 mV s^{-1}. A stable CV curve can be observed after scanning 1000 laps. Then, the OER linear sweep voltammetry (LSV) test was performed at 10 mV s^{-1}. The Tafel diagram is derived from the LSV curve. The electrochemical impendence spectra (EIS) were performed from 100 MHz to 0.1 Hz at the potential of 0.6 V. The electrochemically active surface areas (ECSA) were evaluated by measuring the electrochemical double-layer capacitance (Cdl) via CV at different scan rates (20、40、60、80、100 and 120 mV s^{-1}).

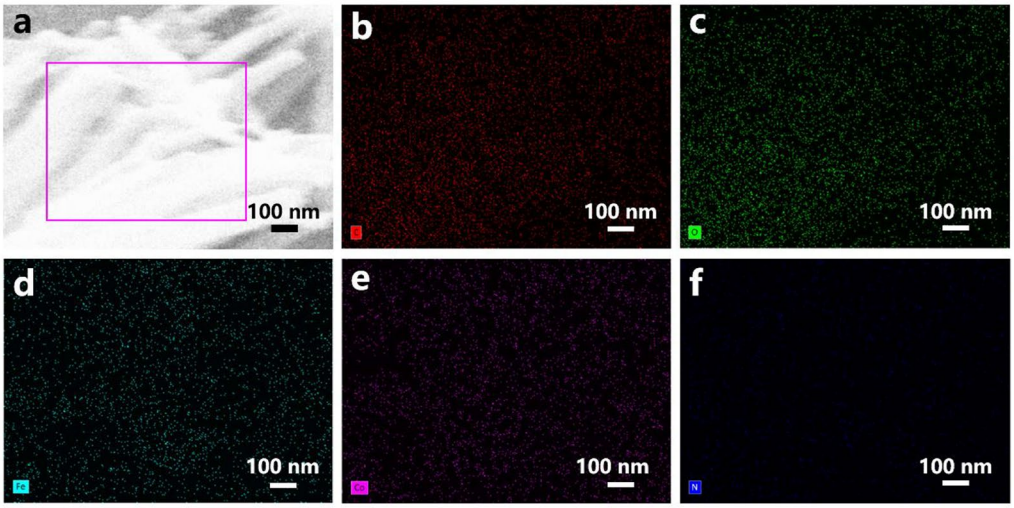

Figure S1. (a) SEM image of FeCo-L_1L_2 and corresponding EDS elemental mapping images of (b) C, (c) O, (d) Fe, (e) Co, (f) N for FeCo-L_1L_2.

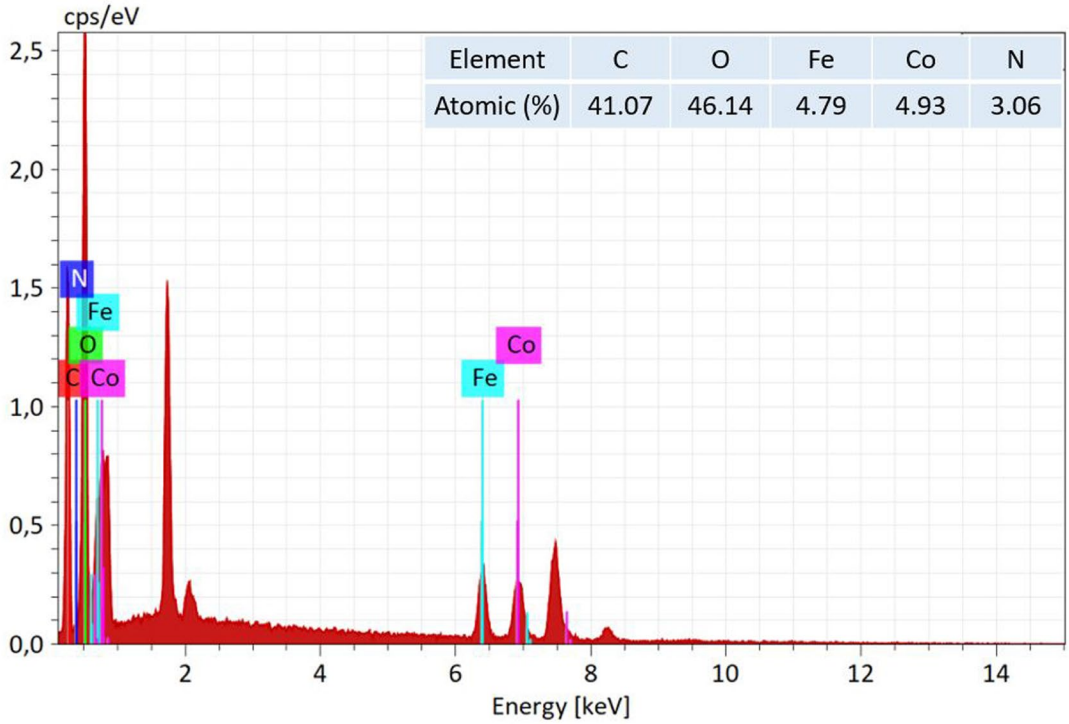

Figure S2. EDS spectrum of FeCo-L_1L_2.

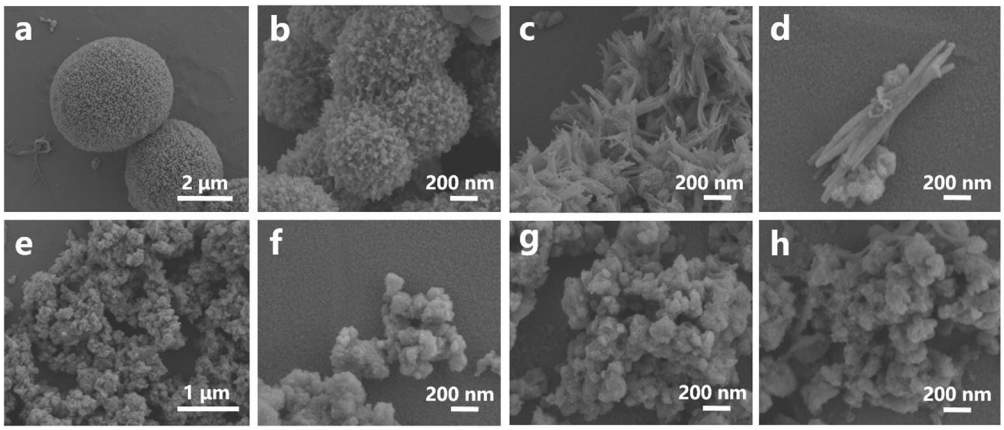

Figure S3. SEM images of (a) $FeCo_9$-L_1L_2, (b) $FeCo_4$-L_1L_2, (c) $FeCo_{2.3}$-L_1L_2, (d) $FeCo_{1.5}$-L_1L_2, (e) $Fe_{1.5}Co$-L_1L_2, (f) $Fe_{2.3}Co$-L_1L_2, (g) Fe_4Co-L_1L_2, (h) Fe_9Co-L_1L_2.

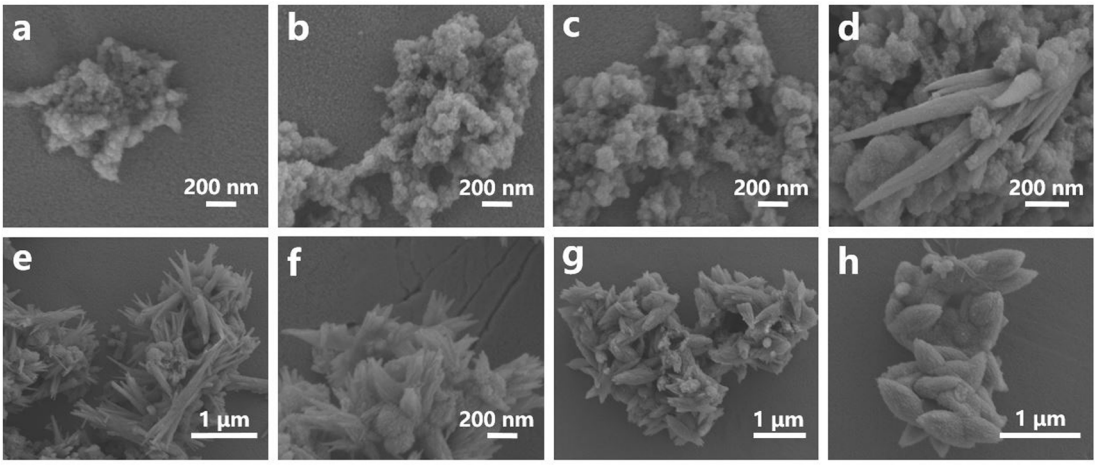

Figure S4. SEM images of (a) FeCo-$L_1L_{2(9)}$, (b) FeCo-$L_1L_{2(4)}$, (c) FeCo-$L_1L_{2(2.3)}$, (d) FeCo-$L_1L_{2(1.5)}$, (e) FeCo-$L_{1(1.5)}L_2$, (f) FeCo-$L_{1(2.3)}L_2$, (g) FeCo-$L_{1(4)}L_2$, (h) FeCo-$L_{1(9)}L_2$.

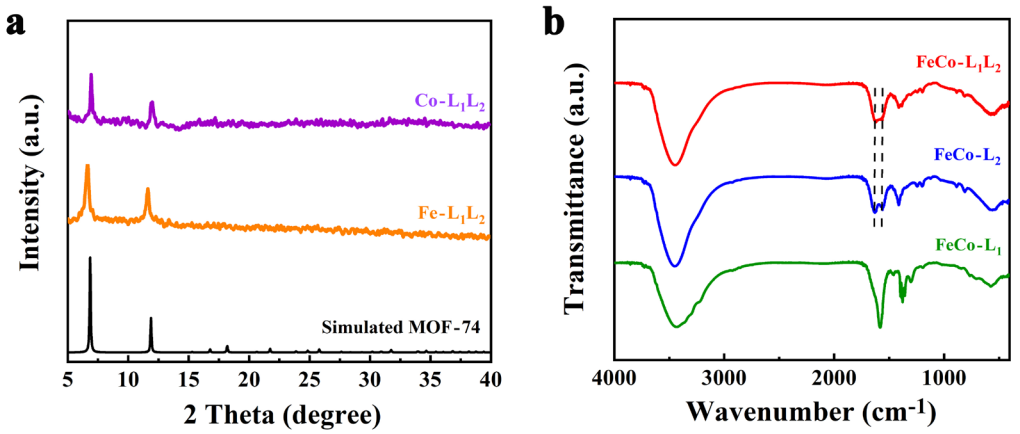

Figure S5. (a) XRD patterns of the as-synthesized Fe-L_1L_2 and Co-L_1L_2 with the corresponding simulated patterns, (b) FT-IR spectra of FeCo-L_1, FeCo-L_2, and FeCo-L_1L_2.

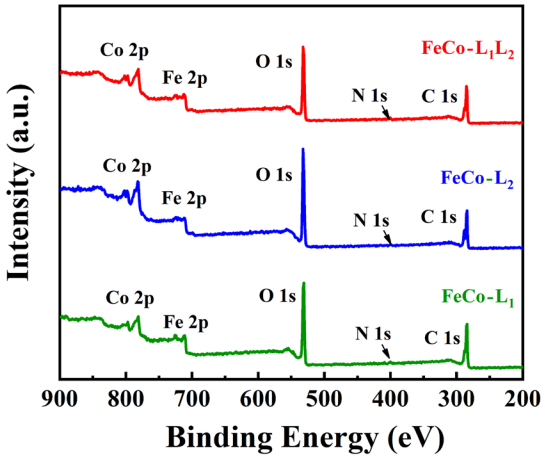

Figure S6. Full range XPS spectra of FeCo-L_1, FeCo-L_2, and FeCo-L_1L_2.

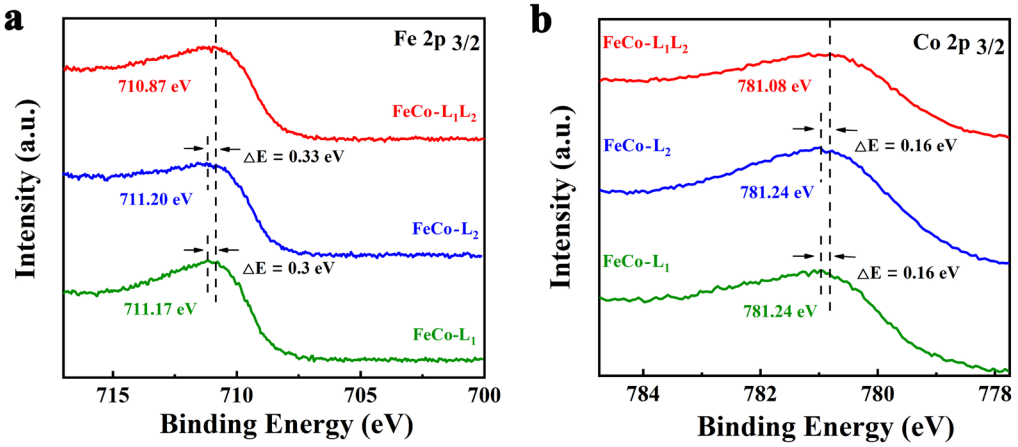

Figure S7. (a) Fe $2p_{3/2}$ spectra, (b) Co $2p_{3/2}$ spectra of FeCo-L_1, FeCo-L_2, and FeCo-L_1L_2.

Table S1. Quantitative analyses of FeCo-L_1, FeCo-L_2, and FeCo-L_1L_2 from XPS.

Sample	Fe (at. %)	Co (at. %)	Fe : Co
FeCo-L_1	5.64	5.40	1.04
FeCo-L_2	5.59	5.75	0.97
FeCo-L_1L_2	5.68	5.53	1.03

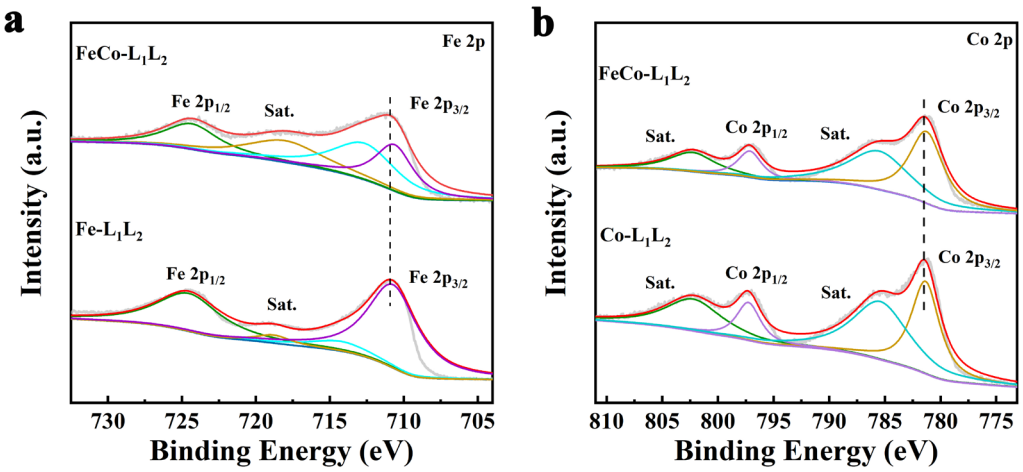

Figure S8. (a) Fe 2p and (b) Co 2p for Fe-L_1L_2, Co-L_1L_2, and FeCo-L_1L_2.

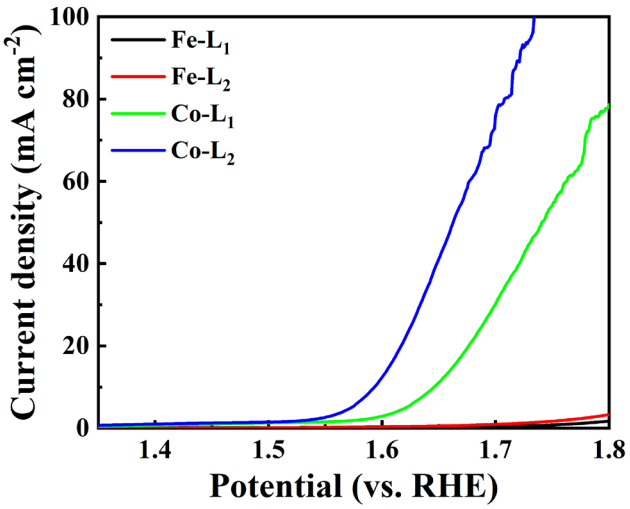

Figure S9. LSV curves of Fe-L_1, Fe-L_2, Co-L_1, and Co-L_2.

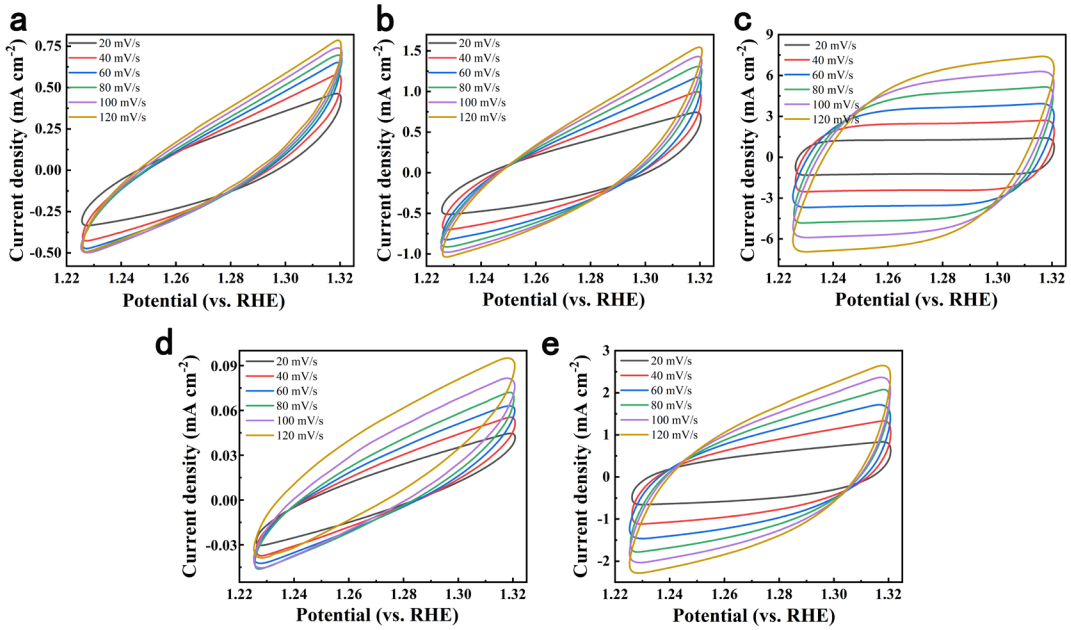

Figure S10. CV plot of (a) FeCo-L_1, (b) FeCo-L_2, (c) FeCo-L_1L_2, (d) Fe-L_1L_2, and (e) Co-L_1L_2 at different scan rate.

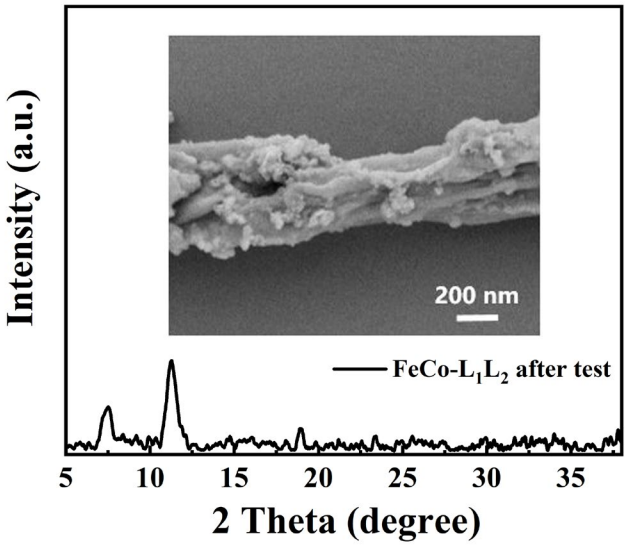

Figure S11. The XRD data and SEM image (inset) of FeCo-L_1L_2 after 10 hours of operation.

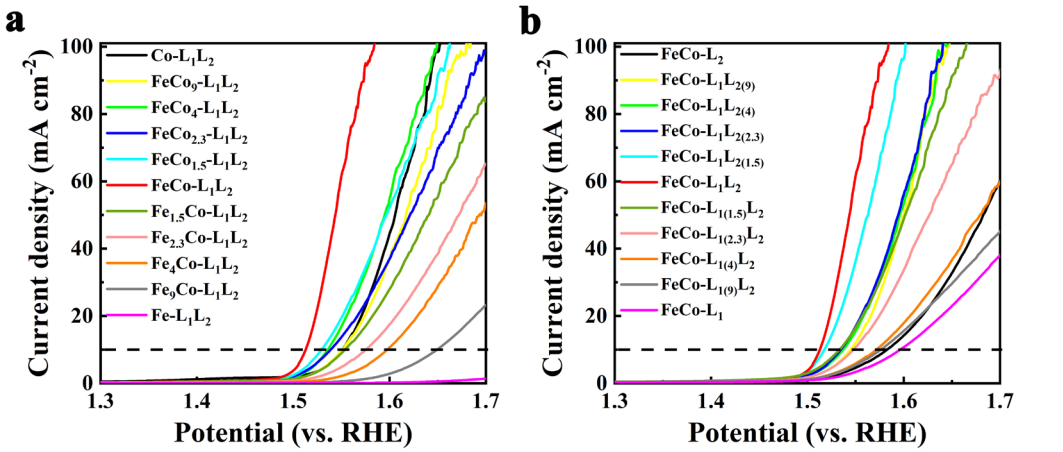

Figure S12. LSV curves of FeCo-L_1L_2 with (a) different metal atom ratios and (b) different ligand ratios.

Table S2. The comparison of electrocatalytic OER performance of FeCo-L_1L_2 with other reported non-precious metal electrocatalysts tested in 1.0 M KOH.

Material	Overpotential at J = 10 mA cm^{-2} (mV)	Tafel slope (mV dec^{-1})	Reference
FeCo-L_1L_2	283.0	31.6	This work
Co-Fe/Ni@HPA-MOF	320.0	58.0	[2]
FeCo-MNS-1.0	298.0	21.6	[3]
CoFe-PYZ(Ni)	300.0	44.0	[4]
Ni-MOF@Fe-MOF	265.0	82.0	[5]
FeNi@CNF	356.0	62.6	[6]
CoFe-LDH	274.0	46.7	[7]
$Ni_{0.75}Fe_{0.25}$BDC	310.0	43.7	[8]
Co-ZIF-9(III)	380.0	55.0	[9]
WCo$Fe_{0.3}$-CNF	254.0	44.8	[10]
Co_3Fe–MOF	280.0	38.0	[11]
$Co_{0.6}Fe_{0.4}$-MOF-74	280.0	56.0	[12]

References

[1] X. Wang, H. Xiao, A. Li, Z. Li, S. Liu, Q. Zhang, Y. Gong, L. Zheng, Y. Zhu, C. Chen, D. Wang, Q. Peng, L. Gu, X. Han, J. Li, Y. Li, *J. Am. Chem. Soc.*, **2018**, *140*, 15336-15341.

[2] M. Lu, Y. Li, P. He, J. Cong, D. Chen, J. Wang, Y. Wu, H. Xu, J. Gao, J. Yao, *J. Solid State Chem.*, **2019**, *272*, 32-37.

[3] L. Zhuang, L. Ge, H. Liu, Z. Jiang, Y. Jia, Z. Li, D. Yang, R. K. Hocking, M. Li, L. Zhang, X. Wang, X. Yao, Z. Zhu, *Angew. Chem. Int. Ed.*, **2019**, *58*, 13565-13572.

[4] J. Gao, J. Cong, Y. Wu, L. Sun, J. Yao, B. Chen, *ACS Appl. Energy Mater.*, **2018**, *1*, 5140-5144.

[5] K. Rui, G. Zhao, Y. Chen, Y. Lin, Q. Zhou, J. Chen, J. Zhu, W. Sun, W. Huang, S. X. Dou, *Adv. Funct. Mater.*, **2018**, *28*, 1801554.

[6] Y. Li, M. Lu, P. He, Y. Wu, J. Wang, D. Chen, H. Xu, J. Gao, J. Yao, *Chem. - Asian J.*, **2019**, *14*, 1590-1594.

[7] M. Cai, Q. Liu, Z. Xue, Y. Li, Y. Fan, A. Huang, M.-R. Li, M. Croft, T. A. Tyson, Z. Ke, G. Li, *J. Mater. Chem. A*, **2020**, *8*, 190-195.

[8] Y. Hao, Q. Liu, Y. Zhou, Z. Yuan, Y. Fan, Z. Ke, C. Y. Su, G. Li, *Energy Environ. Mater.*, **2019**, *2*, 18-21.

[9] K. Jayaramulu, J. Masa, D. M. Morales, O. Tomanec, V. Ranc, M. Petr, P. Wilde, Y. T. Chen, R. Zboril, W. Schuhmann, R. A. Fischer, *Adv. Sci.*, **2018**, *5*, 1801029.

[10] Y. Li, T. Zhao, M. Lu, Y. Wu, Y. Xie, H. Xu, J. Gao, J. Yao, G. Qian, Q. Zhang, *Small*, **2019**, *15*, 1590-1594.

[11] W. Li, W. Fang, C. Wu, K. N. Dinh, H. Ren, L. Zhao, C. Liu, Q. Yan, *J. Mater. Chem. A*, **2020**, *8*, 3658-3666.

[12] X. Zhao, B. Pattengale, D. Fan, Z. Zou, Y. Zhao, J. Du, J. Huang, C. Xu, *ACS Energy Lett.*, **2018**, *3*, 2520-2526.